Tuning Selectivity in Propylene Epoxidation by Plasmon Mediated Photo-Switching of Cu Oxidation State

Andiappan Marimuthu, Jianwen Zhang, Suljo Linic*

Oxidation of functioning copper has restricted its applicability as a catalyst for commercially important epoxidation of propylene to form propylene oxide. Here, we report that steady-state selectivity in propylene epoxidation on copper (Cu) nanoparticles increases sharply when the catalyst is illuminated with visible light. The selectivity increase is accompanied by light-induced reduction of the surface Cu atoms, which is brought about by photoexcitation of the localized surface plasmon resonance (LSPR) of Cu. We discuss multiple mechanisms by which Cu LSPR weakens the Cu-O bonds, reducing Cu_2O.

Heterogeneous catalysts evolve under operating conditions to a steady chemical state that can manifest distinct reactivity from the initial, as-prepared material. For instance, ultrahigh-vacuum (UHV) experiments on well-defined copper (Cu) single-crystal surfaces have shown that metallic Cu exhibits high selectivity to epoxide products in the epoxidation of multiple olefins (*1*–*4*). However, under realistic conditions for commercially critical epoxidation of propylene to form propylene oxide ($C_3H_6 + 1/2O_2 \rightarrow C_3H_6O$), characterized by equimolar amounts of propylene and oxygen and temperature of ~400 to 500 K, Cu is oxidized (*4*–*6*). On the oxidized Cu surface, the selectivity to the desired propylene oxide (PO) product is very low.

We demonstrate an approach to manipulate the oxidation state of Cu catalysts under operating propylene epoxidation conditions and thereby tune the selectivity of the catalyst to favor PO production. The approach takes advantage of the strong interactions of Cu nanoparticles with visible light manifested in the photoexcitation of the localized surface plasmon resonance (LSPR) (*7*–*9*). We find that heterogeneous catalysts containing Cu nanoparticles exhibit a sharp increase in the steady-state selectivity to propylene epoxide from ~20 to ~50% when illuminated with visible light. This increase in the selectivity is accompanied by a light-induced change in the oxidation state of the surface Cu atoms from Cu-oxide (light off) to Cu metal (light on). We find that at a critical light intensity threshold, the change in the product selectivity and Cu oxidation state are observed within less than 2 min, which was the detection limit of our experimental setup.

Catalyst preparation and the experimental setup are described in detail in the supplementary materials. In short, catalysts (12 mg) contained 2 weight percent of Cu nanoparticles, with an average size of 41 ± 9 nm (fig. S1) supported on an inert SiO_2 support and tightly packed into a packed bed reactor. The reactant stream contained equimolar amounts of propylene and oxygen at a total flow rate of 100 cm^3/min and atmospheric pressure. A broadband visible light source with maximum spectral intensity at ~580 nm (fig. S2) and tunable power was used in all experiments. Reaction rates and product selectivity were measured in the differential reactor setup in the regime limited by the reaction kinetics under steady-state reaction conditions.

Steady-state PO selectivity and rate of propylene consumption measured at 473 K as a function of light intensity is shown in Fig. 1A. The data show that the PO selectivity—measured as the rate of generation of PO divided by the rate of generation of all products (equivalent to the rate of consumption of propylene) per unit mass of the Cu catalyst—is ~20% [with the balance consisting of CO_2 and acrolein (fig. S3)] for visible light intensity below ~550 mW/cm^2 (~4 to 5 suns). The selectivity to PO rapidly increases to ~50% as the light intensity crosses the threshold of ~550 mW/cm^2. This is followed by a decrease in the PO selectivity, with a further increase of light intensity, reaching ~35% at ~800 mW/cm^2. The data also show that the reaction rate, measured as the rate of propylene consumption per unit mass of the Cu catalyst, increases for intensities up to 550 mW/cm^2 followed by a sharp decrease at ~550 mW/cm^2 and then an increase for intensity above 550 mW/cm^2. We observed the same threshold behavior for the range of operating temperature between 473 and 553 K.

To obtain an unbiased measure of product selectivity, it is important to measure it at constant rates of propylene consumption. In a steady-state flow reactor, the product selectivity at constant rate is directly proportional to the product yield. At constant temperature and propylene consumption rate, the catalyst illuminated with intensity higher than ~550 mW/cm^2 has higher PO selectivity than that of the catalyst illuminated with intensity below ~550 mW/cm^2 (Fig. 1A). For example, for the propylene consumption rate of ~8 μmol/g/s, measured at intensities of 150 and 550 mW/cm^2, the ~50% PO selectivity for the larger (550 mW/cm^2) intensity is much greater than the only 18% selectivity for the 150 mW/cm^2 intensity. Similarly, for the propylene consumption rates of 25 and 45 μmol/g/s—achieved at (~400 and 700 mW/cm^2) and (450 and 800 mW/cm^2), respectively—the PO selectivity is larger for the light intensity above the 550 mW/cm^2 threshold. This is actually even the case for all reaction rates at constant temperature; the data in Fig. 1A show that the highest measured PO selectivity for the surface illuminated with the intensity below 550 mW/cm^2 is lower than the lowest PO selectivity obtained for intensities above 550 mW/cm^2. In Fig. 1B (as well as figs. S4 and S5), we compared the PO selectivity for the thermal process (no light illumination) with the selectivity on identical catalysts illuminated with the visible light at 550 mW/cm^2 at constant reaction rates. In these experiments, the rate was manipulated by

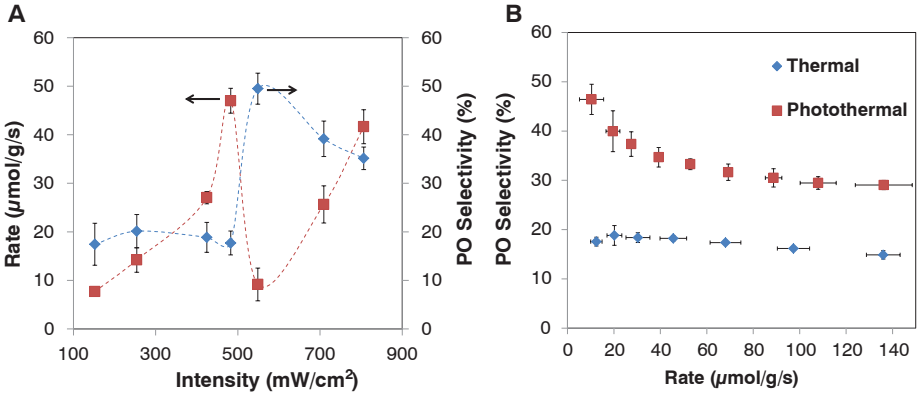

Fig. 1. (**A**) Rate of propylene consumption (left axis, red squares) and the selectivity to PO (right axis, blue diamonds) under photothermal conditions (light on) at 473 K as a function of light intensity. The rate and selectivity data shown in (A) represent the average values of the data obtained from five independent experiments, and the error bars represent SD. (**B**) Selectivity to PO for thermal (light off) and photothermal (light on) processes as a function of the reaction rate. The light intensity used for the photothermal studies was 550 mW/cm^2. The reaction rate and selectivity data shown in (B) represent the average values of the data obtained from three independent experiments, and the error bars represent SD.

Department of Chemical Engineering, University of Michigan, Ann Arbor, MI 48109, USA.

*Corresponding author. E-mail: linic@umich.edu

adjusting the temperature rather than by adjusting the light intensity. The data show that for all measured rates, the steady-state PO selectivity and therefore the PO yield is higher for the illuminated catalyst (light intensity ≥550 mW/cm^2).

The data in Fig. 1 and figs. S3, S4, and S5 show that the steady-state catalytic process undergoes a dramatic change, manifested as a rapid increase in the intrinsic PO selectivity, as the light intensity threshold of ~550 mW/cm^2 is crossed. The data also show that at constant temperature, for the light intensity below ~550 mW/cm^2 the rate of propylene consumption increases with light intensity, followed by a sharp decrease at the threshold of 550 mW/cm^2 and a subsequent increase above the threshold intensity. The light intensity threshold will be affected by multiple factors, including the operating partial pressures of reactants, temperature, and the packing of metallic nanoparticles.

As stated above, UHV studies on model systems have shown that the oxidation state of surface Cu atoms affects the selectivity of Cu-based catalysts in epoxidation reactions, with metallic Cu yielding higher epoxide selectivity than that of the oxidized Cu surface (*1*–*4*). To test whether the light-induced reduction of Cu-oxide to Cu metal might be responsible for the observed increase in the PO selectivity, we characterized the Cu catalysts using in situ ultraviolet-visible (UV-vis) extinction spectroscopy. In Fig. 2A, we show the extinction spectrum of the catalyst, containing nanoparticles of Cu on SiO_2, reduced in 20% H_2 (balance helium) at a temperature of 523 K and atmospheric pressure. It is well established that the extinction peak at ~565 nm is a signature of metallic Cu nanoparticles (fig. S6) (*10*, *11*). The extinction is due to the excitation of the LSPR in metallic Cu nanoparticles. The data also show that as the metallic Cu nanoparticles are exposed to 20% oxygen in helium at 473 K and atmospheric pressure, the LSPR extinction peak is broadened and red shifted, whereas the extinction intensity decreases. These changes in the extinction spectrum upon exposure of Cu nanoparticles to oxygen have been characterized, and it has been shown that they are the result of the formation of a shell of Cu_2O oxide on the metallic Cu core (*10*, *11*). Because of the high sensitivity of Cu LSPR to the local chemical environment, changes in the oxidation state of even a small fraction of Cu surface atoms are accompanied by swubstantial changes in the extinction spectrum (*12*–*14*).

The UV-vis extinction spectrum of the functioning Cu catalyst at steady-state conditions is also shown in Fig. 2A. These catalysts were first prereduced in H_2 and subsequently exposed to operating propylene epoxidation conditions. The data show that as the reactants—equimolar amounts of propylene and oxygen at atmospheric pressure—are introduced at 473 K, the UV-vis extinction spectrum changes from that associated with the metallic Cu to that of the oxidized Cu shell covering the metallic core. Subsequent illumination of the functioning Cu catalyst with UV-vis light of 550 mW/cm^2 intensity results in a dramatic transformation of the catalyst, manifested as the reduction of the Cu-oxide shell. The oxidation (light off) and reduction (light above 550mW/cm^2) of the functioning catalyst take place within 2 min, which is the time required to measure the UV-vis extinction spectrum and well below the time it takes to start making steady-state measurements. As shown in Fig. 1, this light-induced change in the chemical state of surface Cu atoms at 550 mW/cm^2 is accompanied by a dramatic increase in the PO selectivity and a drop in the reaction rate. The conclusion of the in situ UV-vis extinction measurements were further supported by an ex situ analysis of x-ray diffraction (XRD) patterns of the selective (light at 550 mW/cm^2 on) and unselective (light off) catalysts. The unselective catalysts exhibit diffraction features that are consistent with the presence of the Cu_2O shells on Cu, whereas the selective catalysts do not exhibit the oxide diffraction features (Fig. 2B) (*10*).

To further explore the origin of the observed light-induced change in the oxidation state of the Cu catalysts and accompanying changes in the reaction rates and selectivity, we studied the behavior of illuminated, functioning Cu catalysts as a function of the wavelength of incident light. Multiple short- and long-pass optical filters were used to control the wavelength of light reaching the catalysts from the broadband visible light source. The total intensity of light reaching the catalyst was ~550 mW/cm^2 in all experiments, and the operating temperature was 473 K. In the presence of 500-nm long-pass filters (mainly light with wavelengths longer than 500 nm reaching the catalysts), the above-discussed surface transformation from oxidized Cu to metallic Cu takes place (Fig. 3A). On the other hand, as shown in Fig. 3B, when a 500-nm short-pass filter is applied (mainly photons below 500 nm reaching the catalyst) the catalyst is oxidized under the reaction conditions and unperturbed by light. This result suggests a critical role for the Cu LSPR in inducing the chemical transformation of Cu and driving the observed light-induced increase in the PO selectivity because photons with the wavelength below 500 nm do not excite the Cu LSPR.

We propose that the photoexcitation of Cu LSPR, associated with the metallic core of catalytic nanoparticles, serves to reduce the Cu_2O shell at the threshold light intensity of 550 mW/cm^2 and maintain the Cu surface in the metallic state under operating conditions. At this threshold intensity, the material undergoes a dramatic phase change from an oxide to a metal—the material becomes different on the atomic level. Below and above the threshold intensity, the chemical process is taking place on two atomically different surfaces: oxide and metal, respectively. It is this light-induced change in the atomic structure of the surface that causes the dramatic noncontinuous change in the rate of propylene consumption and the intrinsic product selectivity. This noncontinuous change in product selectivity and the rate of propylene consumption observed at the threshold intensity is fundamentally different than the observed variation in the rate and selectivity for intensities below and above the threshold. For light intensities below the threshold, an increase in the intensity results in a continuous increase in the rate of propylene consumption. As is the case in almost any selective partial oxidation reaction, higher conversion of reactant yields higher

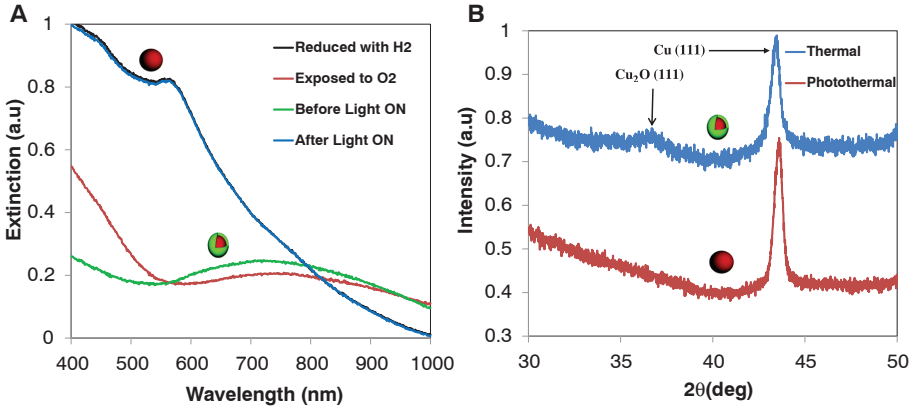

Fig. 2. (**A**) In situ diffuse reflectance UV-vis extinction spectra of the catalyst (2% Cu/SiO_2) reduced with hydrogen at 523 K, exposed to oxygen at 473K, under propylene epoxidation conditions without light (before light on) at 473 K, and under propylene epoxidation conditions with light on (after light on) at 473 K. The light intensity used for the photothermal studies (after light on) was 550 mW/cm^2. The UV-vis extinction spectra of the catalyst reduced with hydrogen and exposed to propylene oxidation under photothermal conditions (after light on) almost completely matched each other. To distinguish these two spectra, the extinction spectrum of the catalyst reduced with hydrogen was scaled by 1.01. a.u., arbitrary units. (**B**) X-ray diffraction spectra for the catalyst used in thermal (light off) and photothermal (light on) studies. The light intensity used for the photothermal studies was 550 mW/cm^2. The arrows indicate the peak positions of Cu(111) and Cu_2O (111) signals.

selectivity to the deep oxidation product CO_2. In this particular case, as the rate of propylene consumption increases, the partial pressures of acrolein and PO in the reactor increase, causing the rate of sequential combustion of these species to increase and yielding higher selectivity to CO_2. The data in Fig. 1A and fig. S3 show that on the Cu oxide surface (intensity below the threshold), the main channel contributing to the increased selectivity to CO_2 at higher rates of propylene consumption involves the sequential oxidation of acrolein—the increase in the CO_2 selectivity is accompanied by a concurrent drop in the acrolein selectivity.

The data in fig. S5 show that a similar effect on the rate of propylene consumption and product selectivity is achieved by increasing the temperature of the Cu oxide surface (light off). This suggests that on the oxide surface, the change in selectivity is only the consequence of the enhanced rate of propylene consumption, and it makes no difference whether the change in the rate is induced by increasing the operating temperature or increasing the intensity of light. Similarly, for light intensities above the threshold an increase in the light intensity also results in an increase in the rate of propylene consumption, therefore increasing the partial pressure of acrolein and PO in the reactor. Again, an increase in the rate of sequential combustion of these species results in higher selectivity to CO_2 as the light intensity is increased. The data in Fig. 1A show that on Cu metal (intensity above the threshold), the main channel contributing to the increased selectivity to CO_2 involves the sequential oxidation of PO. The data in fig. S4 show that a similar effect on the reaction rate and product selectivity is achieved by increasing the temperature of the Cu metal surface.

We also must comment on the mechanism involved in the reduction of the Cu_2O oxide shell. Cu_2O is a semiconductor with a band gap of ~2.0 eV (*15*). There are two mechanisms by which Cu LSPR could induce the reduction of Cu_2O. First, radiative energy transfer from the plasmon Cu states to the oxide shell enhances the rate of electron excitation from the valence (bonding orbitals) to conduction band (antibonding orbitals) of the Cu-oxide shell, weakening the Cu-O chemical bonds in the oxide. This plasmonic energy transfer from an excited plasmonic metal to a nearby semiconductor is well documented (*7*, *16*–*20*). It takes place mainly via dipole-dipole interactions of intense LSPR-mediated electromagnetic fields around the Cu metallic core with the oxide shell. In this mechanism, the metallic Cu core essentially traps light, locally amplifying its effect on the semiconductor (*7*, *16*–*20*). Second, direct LSPR-mediated transient injection of electrons from the metallic Cu core to the antibonding Cu-O orbitals of the oxide shell would also lead to a more facile reduction of Cu-oxide shell. The process has been shown to be functional in many systems in which energetically accessible electronic states (orbitals) interact with metal LSPR. The process of electron injection takes place either directly via chemical interface damping (CID) (*7*–*9*, *21*–*25*) of the metal plasmon states because of their interaction with the antibonding Cu-oxide states, or indirectly through the decay of plasmons into hot electrons (*7*–*9*, *25*–*29*) via Landau damping and subsequent transfer of the energetic electrons to Cu_2O. The observed broadening of LSPR resonance upon the formation of the Cu-oxide shell (Fig. 3) is a clear indication that the imaginary component of the material dialectic function increases, which is direct evidence for the faster rates of LSPR relaxation, most likely owing to the direct injection of electrons into the oxide semiconductor (*21*–*24*). Alternatively, the Cu LSPR might conceivably lead to heating of the Cu particles and their thermal reduction (*25*). This mechanism is not likely because as shown in Fig. 4, if we thermally heat the catalyst (light

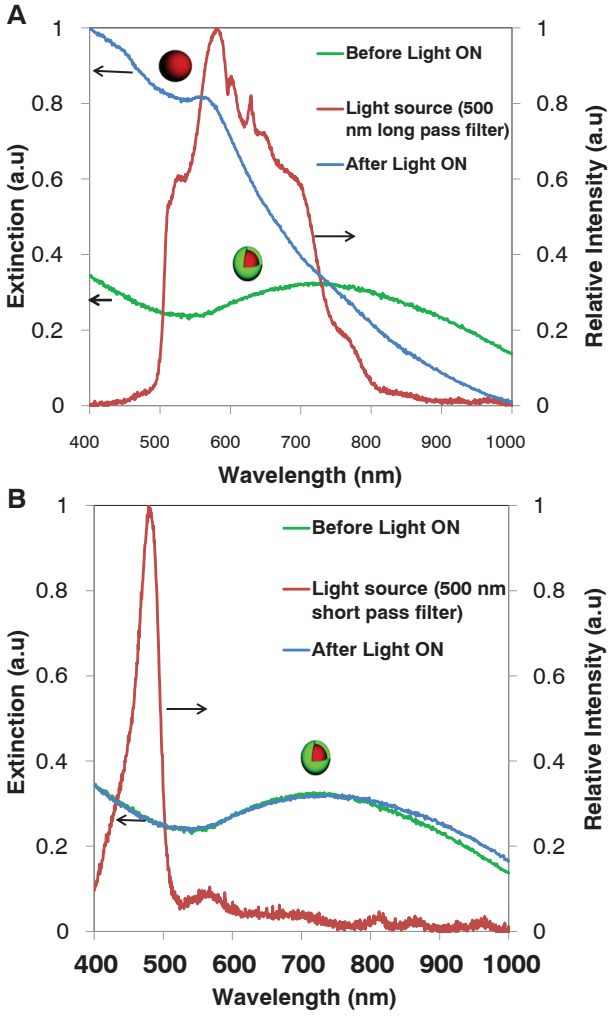

Fig. 3. Spectra of the light source with (**A**) 500-nm long-pass filter and (**B**) 500-nm short-pass filter used in the photothermal studies, superimposed with diffuse reflectance UV-vis extinction spectra of catalyst (2% Cu/SiO_2) measured in situ at 473 K under thermal (before light on) and photothermal (after light on) conditions. The light intensity used for the photothermal studies was 550 mW/cm^2.

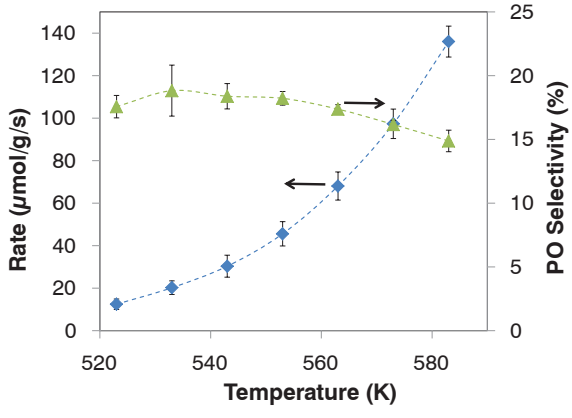

Fig. 4. Rate of propylene consumption (left axis, blue diamonds) and selectivity to PO (right axis, green triangles) under thermal conditions (light off) as a function of temperature. The rate and selectivity data shown in the figure represent the average values of the data obtained from three independent experiments, and the error bars represent SD.

off) the reaction rate steadily increases, and the PO selectivity steadily decreases, as a function of temperature. This behavior is fundamentally different than the behavior observed in response to light (Fig. 1, A and B), in which we see sharp drops in the reaction rate and a sharp increase in the selectivity at ~550 mW/cm^2.

The studies discussed advance a number of critical concepts. Although we focused on Cu nanostructures, the discussed mechanisms are universal, and similar principles could be used in the design of various metal nanomaterials with photo-switchable oxidation states. For example, core-shell nanoparticles containing a plasmonic core (such as Au, Ag, or Cu) and a shell of another metal could lend themselves to similar LSPR-mediated photo-induced switching of the oxidation states of surface atoms. Controlling the oxidation state of functioning catalysts is critical for the control of reactant conversion rates and product selectivity. Second, direct epoxidation of propylene without expensive sacrificial agents is one of the most important processes for which no viable heterogeneous catalyst exists. Although the findings reported here may pave the way toward the discovery of viable heterogeneous propylene epoxidation catalysts, hurdles related to efficient and scalable harvesting of light (including abundant solar light) represent considerable challenges.

References and Notes

1. R. L. Cropley *et al.*, *J. Am. Chem. Soc.* **127**, 6069 (2005).
2. A. K. Santra, J. J. Cowell, R. M. Lambert, *Catal. Lett.* **67**, 87 (2000).
3. J. J. Cowell, A. K. Santra, R. M. Lambert, *J. Am. Chem. Soc.* **122**, 2381 (2000).
4. R. M. Lambert, F. J. Williams, R. L. Cropley, A. Palermo, *J. Mol. Catal. Chem.* **228**, 27 (2005).
5. D. Torres, N. Lopez, F. Illas, R. M. Lambert, *Angew. Chem. Int. Ed.* **46**, 2055 (2007).
6. J. R. Monnier, G. W. Hartley, *J. Catal.* **203**, 253 (2001).
7. S. Linic, P. Christopher, D. B. Ingram, *Nat. Mater.* **10**, 911 (2011).
8. P. Christopher, H. Xin, S. Linic, *Nat. Chem.* **3**, 467 (2011).
9. P. Christopher, H. Xin, A. Marimuthu, S. Linic, *Nat. Mater.* **11**, 1044 (2012).
10. K. P. Rice, E. J. Walker Jr., M. P. Stoykovich, A. E. Saunders, *J. Phys. Chem. C* **115**, 1793 (2011).
11. G. H. Chan, J. Zhao, E. M. Hicks, G. C. Schatz, R. P. Van Duyne, *Nano Lett.* **7**, 1947 (2007).
12. E. M. Larsson, C. Langhammer, I. Zorić, B. Kasemo, *Science* **326**, 1091 (2009).
13. D. Seo, G. Park, H. Song, *J. Am. Chem. Soc.* **134**, 1221 (2012).
14. C. Novo, A. M. Funston, P. Mulvaney, *Nat. Nanotechnol.* **3**, 598 (2008).
15. M. Hara *et al.*, *Chem. Commun. Camb.* 3, 357 (1998).
16. S. K. Cushing *et al.*, *J. Am. Chem. Soc.* **134**, 15033 (2012).
17. P. Christopher, D. B. Ingram, S. Linic, *J. Phys. Chem. C* **114**, 9173 (2010).
18. D. B. Ingram, S. Linic, *J. Am. Chem. Soc.* **133**, 5202 (2011).
19. D. B. Ingram, P. Christopher, J. L. Bauer, S. Linic, *ACS Catal.* **1**, 1441 (2011).
20. K. Awazu *et al.*, *J. Am. Chem. Soc.* **130**, 1676 (2008).
21. U. Kreibig, M. Vollmer, *Optical Properties of Metal Clusters* (Springer, New York, ed. 1, 1995).
22. B. N. J. Persson, *Surf. Sci.* **281**, 153 (1993).
23. U. Kreibig, *Appl. Phys. B* **93**, 79 (2008).
24. H. Hövel, S. Fritz, A. Hilger, U. Kreibig, M. Vollmer, *Phys. Rev. B Condens. Matter* **48**, 18178 (1993).
25. K. Watanabe, D. Menzel, N. Nilius, H.-J. Freund, *Chem. Rev.* **106**, 4301 (2006).
26. L. Brus, *Acc. Chem. Res.* **41**, 1742 (2008).
27. A. M. Michaels, L. Jiang, *J. Phys. Chem. B* **104**, 11965 (2000).
28. A. Furube, L. Du, K. Hara, R. Katoh, M. Tachiya, *J. Am. Chem. Soc.* **129**, 14852 (2007).
29. Y. Tian, T. Tatsuma, *Chem. Commun. (Camb.)* (16): 1810 (2004).

Acknowledgments: We gratefully acknowledge support from the U.S. Department of Energy, Office of Basic Energy Science, Division of Chemical Sciences (FG-02-05ER15686) and National Science Foundation (CBET-0966700, CBET-1132777 and CHE-1111770). S.L. acknowledges the DuPont Young Professor grant by the DuPont corporation and the Camille Dreyfus Teacher-Scholar Award from the Camille & Henry Dreyfus Foundation. We also acknowledge H. Xin for discussions and insight. We declare no competing financial interests.

Supplementary Materials

www.sciencemag.org/cgi/content/full/339/6127/1590/DC1
Materials and Methods
Figs. S1 to S6
References (*30*, *31*)

17 October 2012; accepted 3 January 2013
10.1126/science.1231631

Photoredox Activation for the Direct β-Arylation of Ketones and Aldehydes

Michael T. Pirnot, Danica A. Rankic, David B. C. Martin, David W. C. MacMillan*

The direct β-activation of saturated aldehydes and ketones has long been an elusive transformation. We found that photoredox catalysis in combination with organocatalysis can lead to the transient generation of 5π-electron β-enaminyl radicals from ketones and aldehydes that rapidly couple with cyano-substituted aryl rings at the carbonyl β-position. This mode of activation is suitable for a broad range of carbonyl β-functionalization reactions and is amenable to enantioselective catalysis.

Within the field of organic chemistry, the carbonyl moiety is central to many broadly used synthetic modifications and fragment coupling steps, including Grignard reactions, Wittig olefinations, and reductive aminations. The carbonyl system is also a preeminent activation handle for proximal bond constructions such as α-C=O oxidations, alkylations, arylations, and halogenations (*1*, *2*). However, transformations that allow the direct β-functionalization of saturated ketones and aldehydes remain effectively unknown (*3*, *4*). Herein, we describe a catalysis activation mode that arises from the combination of photoredox and amine catalysis to enable the direct arylation of cyclic and acyclic carbonyls at the β-methylene position (Fig. 1).

Historically, β-carbonyl activation has been limited to the addition of soft nucleophiles to α,β-unsaturated carbonyls. Although the study of such reactivity has delivered many useful transformations, this chemistry requires substrates that are not as widely available or require an additional preoxidation step from a saturated precursor (*5*–*9*). Previous studies in transition metal catalysis have shown that direct β-functionalization of esters or amides is possible through the use of palladium catalysis, albeit with only a few examples known to date (*10*–*13*). A direct aldehyde or ketone β-coupling mechanism would obviate the need for preactivated substrates.

Over the past 4 years, visible light–mediated photoredox catalysis has become a rapidly blossoming research area within the organic and organometallic communities (*14*–*17*). Through a series of photoinduced electron transfer (PET) events, this general strategy allows for the development of bond constructions that are often elusive or currently impossible via classical two-electron pathways. In addition, photoredox catalysis provides an alternative means of generating reactive radical intermediates without operational complexity and toxic precursors (often found with high-energy photochemistry and/or reagent-based radical production).

Recently, using the concept of "accelerated serendipity," our laboratory discovered a unique bond construction that enables the direct arylation of α-methylene amines via visible light photoredox catalysis (*18*). On the basis of mechanistic insights gained from this arylation protocol, we hypothesized that photoredox and amine catalysis might be used in conjunction to enable the direct β-functionalization of carbonyls. A prospective mechanism for this dual-catalysis β-aldehyde or ketone arylation is shown in Fig. 2. It is well known that tris-cyclometalated Ir(III) complexes, such as tris(2-phenylpyridinato-C^2,N)iridium(III) [Ir(ppy)$_3$] (**1**), have a strong absorption cross section in the visible range, allowing them to accept a photon from a variety of light sources to populate the *Ir(ppy)$_3$ (**3**) metal-to-ligand charge transfer excited state (*19*). Given that *Ir(ppy)$_3$ (**3**) is a strong reductant [oxidation potential ($E_{1/2}^{ox}$) = −1.73 V versus saturated calomel electrode (SCE) in CH_3CN] (*19*, *20*), we proposed that this high-energy

Merck Center for Catalysis, Department of Chemistry, Princeton University, Princeton, NJ 08544, USA.

*Corresponding author. E-mail: dmacmill@princeton.edu

Tuning Selectivity in Propylene Epoxidation by Plasmon Mediated Photo-Switching of Cu Oxidation State

Andiappan Marimuthu *et al.*

Science **339**, 1590 (2013);
DOI: 10.1126/science.1231631